Published in final edited form as:
Neurobiol Dis. 2010 April ; 38(1): 17–26. doi:10.1016/j.nbd.2009.12.021.

miR-497 regulates neuronal death in mouse brain after transient focal cerebral ischemia

K.J. Yin, **Z Deng**, **H.R. Huang**, **M. Hamblin**, **C.Q. Xie**, **J.F. Zhang**, and **Y.E. Chen***
Cardiovascular Center, Department of Internal Medicine, University of Michigan Medical Center, Ann Arbor, Michigan 48109, USA

Abstract

Dysfunction of the microRNA (miR) network has been emerging as a major regulator in neurological diseases. However, little is known about the functional significance of unique miRs in ischemic brain damage. Here, we found that miR-497 is induced in mouse brain after transient middle cerebral artery occlusion (MCAO) and mouse N2A neuroblastoma (N2A) cells after Oxygen-Glucose-Deprivation (OGD). Loss-of-miR-497 function significantly suppresses OGD-induced N2A cell death, whereas gain-of-miR-497 function aggravates OGD-induced neuronal loss. Moreover, miR-497 directly binds to the predicted 3'-UTR target sites of bcl-2/-w genes. Furthermore, knockdown of cerebral miR-497 effectively enhances bcl-2/-w protein levels in the ischemic region, attenuates ischemic brain infarction, and improves neurological outcomes in mice after focal cerebral ischemia. Taken together, our data suggest that miR-497 promotes ischemic neuronal death by negatively regulating anti-apoptotic proteins, bcl-2 and bcl-w. We raise the possibility that this pathway may contribute to the pathogenesis of the ischemic brain injury in stroke.

Keywords

microRNAs; apoptosis; bcl-2; bcl-w; cerebral cortex; oxygen-glucose deprivation; cerebral ischemia

INTRODUCTION

Ischemic stroke results from a transient or permanent local reduction of cerebral blood flow, characterized by a set of cellular disturbances. With a mortality rate of 30%, stroke is the third leading cause of death and adult disability in the United States (Goldstein et al., 2001; Kalache and Aboderin, 1995). Unfortunately, development of effective therapies in the clinical setting is seriously limited by the rapid development of brain injury following ischemia (Schellinger et al., 2004; Stapf and Mohr, 2002). Extensive research has demonstrated that stroke triggers complex cellular biochemical events that eventually lead to apoptotic and necrotic neuronal death in the ischemic regions (Love, 2003; Yuan, 2009). However, the delicate mechanisms of stroke-induced neuronal death and neurological dysfunction are not completely understood. Undoubtedly, the elucidation of molecular mechanisms of cell death will provide new insights

*Correspondence addressed to: Y. Eugene Chen, MD, Ph.D. Cardiovascular Center Department of Internal Medicine University of Michigan Medical Center Phone: 734-763-7838 Fax: 734-936-2641 echenum@umich.edu.

into the understanding of cerebral protection aimed at developing neuroprotective agents for stroke therapeutics.

MicroRNAs (miRs) have been recently discovered as a novel family of non-protein coding short RNA molecules that negatively modulate protein expression in various organisms (Bartel, 2009; Bartel and Chen, 2004; Kim, 2005). MiRs hybridize to partially complementary binding sequences that are typically localized in the 3' untranslated regions (3'UTR) of target mRNAs, resulting in either cleavage or translational repression in a sequence-specific manner (Bartel and Chen, 2004). It is now evident that miRs are able to regulate expression of at least one-third of the human genome and play a critical role in a variety of normal biological processes, including cell differentiation, apoptosis, development, and metabolism (Bartel, 2004; Ketting et al., 2001; Lee et al., 2004; Wienholds and Plasterk, 2005). Furthermore, miRs are abundantly expressed in the nervous system and have been initially identified as critical mediators in the regulation of neural development and plasticity (Kosik, 2006).

In addition, miRs have also been implicated in the etiology of a variety of human diseases, including cancer, metabolic diseases, cardiovascular diseases, and viral infections (Care et al., 2007; Krutzfeldt and Stoffel, 2006; Sullivan and Ganem, 2005; Wiemer, 2007). Accumulating evidence has linked dysregulated cerebral miR expression to a variety of neurodegenerative diseases, including Alzheimer's disease (Hebert et al., 2008), Parkinson's disease (Kim et al., 2007) and stroke (Dharap et al., 2009; Jeyaseelan et al., 2007).

Recently, a few groups have shown the involvement of miRs in the pathogenesis of ischemic brain injury by using miR profiling techniques in a rat middle cerebral artery occlusion (MCAO) model (Dharap et al., 2009; Jeyaseelan et al., 2007). These findings suggest several miRs as potential candidates for possible biomarkers or therapeutic targets in stroke. However, there are no studies available to date that investigate the functional significance and molecular mechanisms of individual microRNAs in post-ischemic neuronal death. In this article, we have first identified cerebral miR-497 as a critical player in the regulation of ischemic neuronal death in N2A neuroblastoma cells and also in a mouse MCAO model. We have further demonstrated that miR-497 directly targets anti-apoptotic genes, bcl-2 and bcl-w to trigger ischemic brain damage.

MATERIALS AND METHODS

All chemicals and reagents were purchased from Sigma-Aldrich (St. Louis, MO), while cell culture supplies were purchased from Invitrogen Corporation (Carlsbad, CA) unless specified.

Mouse model of transient focal cerebral ischemia

Male C57/B6 mice were purchased from Jackson Laboratory. Focal cerebral ischemia was induced by intraluminal middle cerebral artery occlusion (MCAO) using a nylon monofilament suture as described previously (Yang et al., 1997). Briefly, mice were anesthetized with ketamine (100mg/kg) and xylazine (10 mg/kg). After a midline skin incision, the left common carotid artery was exposed and then its branches were electrocoagulated. A 2-cm length of 6–0 rounded tip nylon suture was gently advanced from the external carotid artery up to the internal carotid artery until regional cerebral blood flow (rCBF) was reduced to less than 16 % of baseline. After 60 minutes of proximal MCA occlusion, blood flow was restored by removing the suture. Changes in cerebral blood flow (CBF) at the surface of the cortex were recorded using a laser-Doppler flowmetry monitor (BPM2 System, Vasamedic, St. Paul, MN). Sham control animals were subjected to similar operations to expose the carotid arteries without occlusion of the middle cerebral artery. After 60 minutes of MCAO, the mice were allowed to recover for 24 hours. Arterial blood gases, mean arterial pressure, and heart rate were also monitored in selected animals 30 min before, during, and 30 min after MCAO. The rectal

temperature was controlled at 37.0 ± 0.5°C during surgery with a feedback-regulated heating pad (Harvard, Holliston, MA). After the ischemic insult, mice were kept in an air-ventilated incubator at 24.0±0.5°C. The animals were sacrificed at 24 h of reperfusion, and the brains were quickly removed for biochemical assays as well as infarct determination. All procedures using laboratory animals were approved by the University of Michigan Animal Care and Use Committee.

N2A cell culture and oxygen-glucose deprivation (OGD)

Mouse N2A neuroblastoma cells were purchased from American Type Culture Collection (ATCC, Manassas, VA) and were grown to 60% confluence in a 1:1 mixture of DMEM and Ham's F-12K medium supplemented with 10% FBS. To mimic ischemic-like conditions *in vitro*, cell cultures were exposed to OGD for several hours and then returned to 95% air, 5% CO_2, and glucose-containing medium for different recovery times (Yin et al., 2002a). Mouse N2A neuroblastoma cells were transferred into a temperature controlled (37±1°C) anaerobic chamber (Forma Scientific, Marietta, OH) containing a gas mixture composed of 5% CO_2, 95%N_2. The culture medium was replaced with deoxygenated glucose-free Hanks' Balanced Salt Solution (Invitrogen, Carlsbad, CA)) and cells were maintained in the hypoxic chamber for 3 h. After OGD, N2A cells were maintained in glucose-containing Hanks' balanced salt solution under normoxic culture conditions for 0, 4, and 24 h. Control mouse N2A neuroblastoma cells were not exposed to OGD.

Treatment of N2A cells with miR-497 mimic or inhibitor

In specific experiments, mouse N2A cells were plated in 24-well or 6-well multi-well plates and were transfected with a miR-497 mimic or mimic control at a final concentration of 50 nM (miRIDIAN mimic, Dharmacon, Chicago, IL) using Lipofectamine 2000 (Invitrogen) according to the manufacturer's instructions. After 48h, the cells were then subjected to OGD and harvested for cell death assay or western blot studies.

Intracerebroventricular infusion of miR-497 antagomir

The procedure was performed as previously described (Dharap et al., 2009). Briefly, C57/B6 mice were anesthetized and fixed in a stereotaxic apparatus. The brain infusion cannula was stereotaxically implanted into the left lateral ventricle of the brain (Bregma: −0.22 mm; Dorsoventral: 3 mm; Lateral: 1 mm)(Paxinos et al., 1985), and was affixed to the skull. The micro-osmotic pump (Alzet 1003D, DURECT corporation, Cupertino, CA) connected with a brain infusion cannula was placed in a subcutaneous pocket on the neck of the mouse. Continuous intracerebroventricular infusion of a miR-497 antagomir, miR-antagomir negative control (eGFP mRNA antagomir) (20 pmol/ul, at a rate of 1 ul/h) or vehicle (artificial CSF) was started 2 days prior to MCA occlusion. Transient focal cerebral ischemia was induced in the left MCA territory for 1 h and all mice were sacrificed 1 day after MCA occlusion. Mouse brains were removed and then subjected to TTC staining for measurement of infarct volume (n=9), western blot for bcl-2 and bcl-w (n=3), and quantitative PCR for miR-497 or miR-21 levels (n=3). The antagomirs are antisense oligonucleotides for individual miRNA and modified at each nucleotide by an O-*methyl* moiety at the 2-ribose position. These antisense oligonucleotides were synthesized by Integrated DNA Technologies (Coralville, IA) with the following sequence and structure: miR-497 antagomir: 5'-mUmAmCmAmAmAmCmCmAmCmAmGmUmGmUmGmCmU mGmCmUmG -3'; eGFP mRNA antagomir: 5'-mAmAmGmGmCmAmAmGmCmUmGmAmCmCmCmUmGmAmAmGmU-3'. All antagomirs were filled into micro-osmotic minipumps, and incubated at 37°C overnight before implantation.

Assessment of mouse N2A cell death

The extent of N2A cell death was assessed by the 3-(4, 5-*dimethylthiazol*-2-*yl*)-2, 5-*diphenyl-tetrazolium bromide* (MTT) and LDH assays as described previously (Yin et al., 2002a; Yin et al., 2002b).

Quantitative real-time PCR

Total RNA, including miRs was isolated from cerebral cortex or N2A cell cultures by using a miRNeasy Mini Kit (Qiagen, Valencia, CA). Reverse transcription was performed using the TaqMan MiRNA Reverse Transcription Kit (Applied Biosystems, Foster City, CA). Equal amounts of total RNA (10 ng) were reverse-transcribed with 100 mM dNTPs (with dTTP), 50 U reverse transcriptase, 0.4 U RNase inhibitor, and specific microRNA reverse transcriptase primers at a condition of 16°C for 30 mins, 42°C for 30 mins, and 85°C for 5 mins. PCR reactions were then conducted using the TaqMan® MiRNA Assay Kit (Applied Biosystems) at 95°C for 10 mins, followed by 40 cycles of 95°C for 15 sec and 60°C for 1 min. Each PCR reaction contained 1.33 μl of the RT reaction product, 10 μl TaqMan 2 × Universal PCR Master Mix, 1 μl 20 × TaqMan® MicroRNA Assay reagent in a total volume of 20 μl. The relative microRNA levels were normalized to endogenous SnoRNA 202 expression for each sample. The PCR experiments were repeated 3 times, each using separate sets of cultures (Yin et al., 2006a; Yin et al., 2006b).

Western blot analysis

Total protein was isolated from the cerebral cortex or N2A cells as described previously (Yin et al., 2006a; Yin et al., 2006b). Samples (20–40μg of protein) were electrophoresed onto a 10–15% SDS/polyacrylamide gel (SDS/PAGE), and transferred to PVDF membranes. The membranes were blocked in TBS-Tween buffer containing 20 mM Tris-HCl, 5% nonfat milk, 150 mM NaCl, and 0.05% Tween-20 (pH 7.5) for 1 h at room temperature. Thereafter, the blot was incubated with primary rabbit anti-Bcl-2 antibody (1:1000; Santa Cruz, CA), rabbit anti-Bcl-w antibody (1:1000; Cell Signaling, Danvers, MA), or mouse anti-actin antiserum (1:500; Santa Cruz, CA) for 1–2 h at room temperature. The membrane was washed with TBST 3 times at 10 min intervals, incubated with the secondary antibody (1:5000; anti-rabbit, anti-mouse or anti-goat IgG conjugated with alkaline phosphatase, Promega; Madison, WI) at RT for 1 h, then washed 3 times each at 10 min intervals with TBST and 2 times each for 10 min with TBS. The color reaction was developed by the Blot AP System according to the technical manual provided by Promega (Madison, WI).

Plasmid construction

A 566 bp segment from the 3'UTR of the bcl-2 gene or a 746 bp segment from the 3'UTR of the bcl-w gene containing miR-497 binding sites was amplified by PCR from mouse genomic DNA and then cloned into the *Sac* I/*Hind* III site of pMIR-REPORT Luciferase vector (Applied Biosystems). The following primer sets were used to generate specific fragments: bcl-2-UTR Forward, 5'-AGAGCTCGCCTTCAGAGGGTTGCTT-3', bcl-2-UTR Reverse, 5'-CAAGCTTTACTGTCCAGTTCTAGGGTCC-3'; bcl-w-UTR Forward, 5'-AGAGCTCAGAGTACCTGCCATGACCTAA-3', bcl-w-UTR Reverse, 5'-CAAGCTTGCAAAGCCCTTACCACA-3'. We also generated a mutant 3'UTR of the bcl-2 and bcl-w genes with substitutions of 3 bp respectively from the site of perfect complementarity by using the QuikChange XL Site-Directed Mutagenesis Kit (Stratagene). The sequence of mutant bcl-2 or bcl-w 3'UTR segments contained 5'-gaataagaaaccctgtg***GCC***ctatcctgccaagatcattg-3' or 5'-ccaaggtgctaacattg***GCC***ctctttaatgctgacttcg-3' respectively (the three italic bold nucleotides are mutated). Both wild-type and mutant inserts were confirmed by sequencing.

Luciferase assays

Mouse N2A cells were plated at 0.5×10^5 cells per well in 24-well plates. The following day, cells were co-transfected with 800 ng pMIR-REPORT Luciferase vector, including the 3'UTR of bcl-2 or bcl-w (with either wild-type or mutant miR-497 binding sites), and miR-497 mimic or mimic control at a final concentration of 50 nM by using Lipofectamine 2000 (Invitrogen). Luciferase assays were performed by using the dual luciferase reporter assay system (Promega) 48 h after transfection.

Measurement of infarct volume and neurological deficit

Infarct volume was measured using 2% 2,3,5-*triphenyltetrazolium chloride* (TTC) staining as described previously. Mouse brains were removed at 24 h after MCAO, and sliced into 8 coronal sections (1 mm thick) by a mouse brain matrix. The slices were stained with 2% TTC for 15 min at 37°C, scanned and the infarct area was estimated by Metamorph software. The infarct volume was calculated using a derived formula (Swanson et al., 1990) in which infarct volume as a percentage of the contralateral hemisphere was calculated as 100 (contralateral hemisphere volume – non-infarct ipsilateral hemisphere volume)/contralateral hemisphere volume.

Following cerebral ischemia, mice were also tested for neurological deficits and scored on a 5-point scale (Vemuganti et al., 2004): 0, no observable neurological deficits (normal); 1, failure to extend right forepaw (mild); 2, circling to the contralateral side (moderate); 3, falling to the right (severe). 4, mice could not walk spontaneously; depressed level of consciousness (very severe).

Quantitative and Statistical analysis

Quantitative analysis of selected bands in western blots was performed using the NIH Image Analysis System.

Quantitative data were expressed as mean ± SD based on at least 3 separate experiments of triplicate samples. Differences among groups were statistically analyzed by one-way analysis of variance followed by Bonferroni's post-hoc test. Comparison between two experimental groups was based on a two-tailed t-test. A p-value less than 0.05 was considered significant.

RESULTS

The expression of miRs is changed in mouse brain after transient focal cerebral ischemia

After PCR profiling of 40 mouse miRs in the mouse cerebral cortex, only four miRs (miR-497, miR-424, miR-1 and miR-7) exhibit a significantly changed expression at the 24 h reperfusion time point after transient MCAO compared with the sham group (Data not shown and Fig. 1A). MiR-497 shows a nearly 4-fold increase at 24 h-reperfusion (Fig. 1A) and therefore was chosen for further characterization in this study.

Altered miR-497 expression regulates OGD-induced cell death in mouse N2A cells

MiR-497 expression was also tested in mouse N2A cells after OGD (Fig. 1B). The increase in miR-497 is evident from the beginning of cell recovery and persists up to 24h following 3h OGD. OGD-induced cell death was simultaneously assayed by LDH and MTT methods. As indicated in Fig. 1, 3h of OGD exposure does not result in obvious N2A cell death. However, neuronal death appears to dramatically increase at the 4h recovery time point following 3h OGD and persists for at least 24 h (Fig. 1C, D). Clearly, miR-497 upregulation occurs prior to OGD-induced cell death.

To further explore the contributory role of miR-497 in the regulation of OGD-induced N2A cell death, gain- or loss-of-miR-497 function was achieved by transfecting a miR-497 mimic or inhibitor reagent into N2A cells. As demonstrated in Fig. 2, treatment with a miR-497 mimic increases N2A cell death in both non-OGD and OGD conditions (Fig. 2C, D), whereas the miR-497 inhibitor effectively reduces OGD-induced N2A cell death compared to control groups (Fig. 2A, B). These results demonstrate that *in vitro* ischemic-like stimuli induce miR-497 expression, resulting in neuronal death.

Bcl-2 and Bcl-w are target genes of miR-497 in mouse N2A cells after OGD

Recent research has revealed that apoptosis plays a critical role in neuronal death in the ischemic penumbra after focal cerebral ischemia (Love, 2003; Yuan, 2009). An increasing number of studies have provided strong evidence that Bcl-2 family members, bcl-2 and bcl-w, are key regulators in attenuating stroke-induced apoptotic cell death (Chen et al., 2000; Linnik et al., 1995; Martinou et al., 1994; Sun et al., 2003).

Using bioinformatics analysis, we found a conserved miR-497 binding site within the 3'UTRs of bcl-2 and bcl-w, implying that miR-497 may repress translation of these proteins. Consistent with this hypothesis, we note that both bcl-2 and bcl-w protein levels are decreased, with reduced levels beginning at the 4h recovery time point and persisting up to 24 h in N2A cells after 3h of OGD stimuli (Fig. 3A).

To confirm the contributory role of miR-497 in the regulation of bcl-2 and bcl-w, both *in vitro* gain- and loss- of-miR-497 function methods were applied by transfecting N2A cells with a miR-497 mimic or inhibitor reagent. As shown in Fig. 3, miR-497 inhibitor effectively increases (Fig. 3B), whereas miR-497 mimic decreases (Fig. 3C) the expression of bcl-2 and bcl-w in mouse N2A cells subjected to 3h OGD followed by 4 h of recovery time. Of note, the miR-497 mimic or inhibitor has no effect on the expression of bcl-xl, another member of the antiapoptotic bcl-2 family of proteins, suggesting the specificity of miR-497 suppression on bcl-2 and bcl-w.

To further verify that miR-497 may repress bcl-2 and bcl-w through direct interaction with predicted binding sites located in the 3'-UTR region of these proteins, we cloned a reporter vector in which CMV driven-luciferase cDNA was followed by a fragment of the 3'-UTR from both bcl-2 and bcl-w mRNA containing the putative miR-497 binding sequences (Fig. 4). We also generated a luciferase reporter construct fused to the bcl-2 and bcl-w 3'-UTRs, but with a mutant miR-497 binding sequence (Fig. 4). We then transfected this luciferase reporter vector with either wild-type or mutant miR-497 binding sequences into N2A cells. We also co-transfected these cells with a miR-497 mimic or mimic control and measured luciferase activity. As shown in Fig. 4, the miR-497 mimic administered at a concentration of 50nM decreases luciferase activity of the reporter vector containing miR-497 binding sequences (Fig. 4). As expected, the miR-497 mimic has no significant effect on the reporter vector with mutated miR-497 binding sequences. Taken together, these results suggest that miR-497 decreases bcl-2 and bcl-w mRNA translation by directly acting on response elements specific for miR-497 in the bcl-2 and bcl-w 3'-UTR regions.

Inhibition of miR-497 increases bcl-2 and bcl-w levels in vivo, and attenuates ischemic brain damage

We noticed that bcl-2 and bcl-w protein expression levels are significantly reduced in mouse cerebral cortex 24 h after MCAO (Fig. 5A). This is consistent with the idea that ischemia-induced elevation in miR-497 levels negatively regulates expression of these proteins. To further determine the possible role of miR-497 in ischemic brain injury *in vivo*, we employed a micro mini-pump technique to continuously deliver a miR-497 antagomir, eGFP mRNA

antagomir (20 pmol/μl, at a rate of 1μl/h), or artificial CSF into the cerebral lateral ventricle. As shown in Fig. 5B, successful knockdown of miR-497 levels in the cerebral cortex by a specific miR-497 antagomir is confirmed by quantitative PCR. A miR-antagomir negative control (eGFP mRNA antagomir) and vehicle control (artificial CSF) were also similarly tested and neither has any effect on miR-497 expression. As expected, the miR-497 antagomir also has no effect on the expression of another microRNA, miR-21, suggesting the specificity of this technique (Fig. 5B). Compared to both controls, treatment with the miR-497 antagomir significantly reverses ischemia-induced reduction of bcl-2 and bcl-w but not bcl-xl protein levels, suggesting bcl-2 and bcl-w are target genes of miR-497 in mouse brain after focal cerebral ischemia (Fig. 5C). Consequently, knockdown of miR-497 effectively attenuates ischemic brain infarction in cerebral cortex and subcortical areas (Figs.6A and 6B–D) and improves neurological deficit (Fig. 6E). Of note, the cerebral protective effect of the miR497 antagomir was more prominent in the cortex (Fig. 6C) than in the subcortex (Fig. 6D). These data demonstrate that inhibition of cerebral miR-497 provides a neuroprotective role in ischemic brain insult by targeting anti-apoptotic proteins, bcl-2 and bcl-w.

DISCUSSION

The major finding of our study is that miR-497 inhibits bcl-2 and bcl-w expression and exacerbates neuronal death in ischemic insults (Fig. 6F). For the first time, our data suggest that an individual microRNA can regulate translation of several putative antiapoptotic bcl-2 family proteins through gene silencing and modulating stroke-induced brain injury.

Over the last decade, it has been well-demonstrated that many neurons in the ischemic areas undergo necrotic and apoptotic cell death after a stroke event (Love, 2003; Yuan, 2009). In contrast to necrosis, apoptosis appears to be an orderly, programmed cell death. Two general signaling cascades, the mitochondria and cell death receptor-mediated pathways, have been identified for activation of apoptosis in cerebral ischemia (Love, 2003; Yuan, 2009). The bcl-2 family of proteins has been found to participate in these complicated apoptotic signaling pathways. Members of the bcl-2 family have either pro-or anti-apoptotic functional capabilities and have been studied extensively for the past two decades (Youle and Strasser, 2008). Bcl-2 family members have been traditionally classified under three subsets. One class inhibits apoptosis (Bcl-2, Bcl-xl, Bcl-w, Mcl1, and A1), whereas a second class promotes apoptosis (Bax, Bak and Bok). Interestingly, the third specific class, known as BH3-only proteins (Bad, Bim, Bid, DP5, Bik, Bmf, Noxa, and Puma), has a conserved BH3 domain that can bind and regulate the anti-apoptotic bcl-2 proteins and promote apoptosis (Youle and Strasser, 2008). Bcl-2 and bcl-w levels are initially decreased in cerebral ischemia (Webster et al., 2006). Consequently, it has been observed that bcl-2 transgenic mice or viral vector-mediated overexpression of bcl-2 or bcl-w levels in mouse brains have a smaller lesion size compared to wild-type control mice after focal cerebral ischemia (Linnik et al., 1995; Martinou et al., 1994; Sun et al., 2003). In contrast, the occurrence of a stroke in bcl-2 knockout mice or animals treated with antisense oligonucleotides that suppress bcl-2 results in an increased infarct volume (Chen et al., 2000; Hata et al., 1999). These studies clearly suggest bcl-2 and bcl-w have a neuroprotective role in response to cerebral ischemia. Consistent with the previous reports, in this study, we also observed that both bcl-2 and bcl-w protein levels are significantly downregulated in neuronal cell cultures after OGD exposure as well as in mouse brain after 24 h of reperfusion following MCA occlusion. Furthermore, we found that regulation of these two anti-apoptotic proteins by miR-497, an apoptosis-related microRNA, may potentially affect their neuroprotective functions against stroke.

The discovery of microRNAs (miRs) that mediate post-transcriptional silencing of specific target genes has shed light on how non-coding RNAs can play important roles in apoptosis. An increasing number of miRs have recently been found to regulate pro-and anti-apoptotic

genes in apoptotic signaling pathways (Jovanovic and Hengartner, 2006; Schickel et al., 2008). In mammalian cells, several miRs such as miR-21 and the miR-17–92 cluster have been reported as anti-apoptotic molecules in various cancer cells (Frankel et al., 2008; Hayashita et al., 2005; Meng et al., 2007). By contrast, miR-15a, miR-16 and miR-29 represent another class of miRs that promote apoptosis (Cimmino et al., 2005; Mott et al., 2007). In our study, we found OGD-induced elevation in miR-497 expression levels in N2A cell cultures is associated with increased neuronal death. Increasing levels of miR-497 are also evident in mouse cerebral cortex in the MCA territory after transient focal cerebral ischemia. *In vitro* loss- or gain-of-miR-497 function results in reduced or increased cell death respectively. Furthermore, continuous delivery of the miR-497 antagomir to mouse lateral cerebral ventricles effectively reduces brain infarction and improves neurological outcomes after focal ischemia. Our data has unveiled miR-497 as a novel pro-apoptotic regulator and contributes to the pathogenesis of focal cerebral ischemia. To our knowledge, this is the first apoptosis-related microRNA reported to have a critical role in the regulation of ischemic neuronal death.

MiRs are novel, short non-coding RNAs that regulate gene expression at post-transcriptional and/or translational levels. The mature miRs can bind to the 3' untranslated region (3'-UTR) of its target gene mRNA to generate either mRNA degradation (for perfect complementary base-paring) or protein translation inhibition (for imperfect complementary base-pairing) (Bartel and Chen, 2004; Kim, 2005). Recently, several software programs such as targetscan, pictar, and miranda have been developed as very useful tools for performing miR target prediction (Kuhn et al., 2008). In this study, we have shown that miR-497 expression is inversely correlated with bcl-2 and bcl-w expression in N2A cells and also in ischemic mouse cerebral cortex, suggesting a negative regulation of miR-497 regarding the translation of these two anti-apoptotic genes. In order to examine the mechanism responsible for this inhibitory effect, we have conducted a bioinformatics search for the 3'-UTRs of bcl-2 and bcl-w with potential miR-497 binding sites. Indeed, we have found that both bcl-2 and bcl-w 3'-UTR regions contain one potential binding site for miR-497. Moreover, fusion of the bcl-2 or bcl-w 3'-UTR to the luciferase reporter vector results in functional expression in cultured neuronal cells and this activity is markedly suppressed with treatment of exogenous miR-497. However, mutations of several core sequences in the potential miR-497 binding site in bcl-2 and bcl-w 3'-UTRs nearly abolishes this luciferase activity. Furthermore, upregulation of miR-497 results in a stronger reduction of bcl-2 and bcl-w expression after OGD exposure, whereas downregulation of miR-497 increases bcl-2 and bcl-w translation. Taken together, our data demonstrate that miR-497 can directly bind to the 3'-UTRs of bcl-2 and bcl-w, and repress their translation.

Recently, two studies have identified altered expression of several miRs in rat brains after focal cerebral ischemia. Through the use of microarrays, these reports demonstrate the potential importance of miR dysfunction in the pathogenesis of stroke. These studies show that expression levels of specific miRs can either increase or decrease after MCAO. Moreover, the change in expression of certain miRs is associated with different reperfusion times following MCAO (Dharap et al., 2009; Jeyaseelan et al., 2007). In the present study, we used quantitative RT-PCR to evaluate the importance of 36 specific miRNAs in mouse brains subjected to 24h reperfusion time after MCAO. These miRs were previously shown to display highly-altered expression in rat cerebral cortex (Jeyaseelan et al., 2007). However, we found only three miRs with altered expression (two increased and one decreased) in mouse ischemic brain. This inconsistency may be derived from differences in experimental animals, reperfusion time and number of miRs investigated. However, consistent with Jeyaseelan *et al.*, we also observed that miR-497 has a 4–5 fold increase in mouse brain after the same ischemic insult. Moreover, we have extended these previous studies and examined the importance of miR-497 in the regulation of ischemia-induced neuronal death. Indeed, we further demonstrate that miR-497 can directly hybridize to the 3'-UTR of bcl-2 and bcl-w genes and inhibit translation. In

addition, our laboratory utilized similar cerebroventricular antagomir infusion methods previously reported (Dharap et al., 2009) and we have demonstrated that inhibition of miR-497 *in vivo* effectively supresses miR-497 levels, reduces ischemic infarction, and improves neurological deficits by reversing ischemia-induced reduction of bcl-2 and bcl-w.

The role of miRs in stroke studies is largely unknown, and many individual targets of miRs within ischemic neural cells have not yet been identified. The elucidation of miR mechanisms involved in neuronal death may be important for understanding the pathogenesis of cerebral ischemia. Our present data suggest an altered expression profile of cerebral miRs in mouse stroke models. We have also demonstrated that miR-497 is induced by ischemia and contributes to the pathogenesis of ischemic brain injury by directly targeting two antiapoptotic genes, bcl-2 and bcl-w. Thus, inhibition of miR-497 may become a potential therapeutic option for stroke-related brain damage. However, further studies using neuron-specific miR-497 transgenic and knockout animal models are necessary to further validate the detrimental role of miR-497. Finally, the upstream regulation of miR-497 by transcriptional factors must also be investigated in order to fully understand the stroke-related function of this particular miR.

Acknowledgments

This work was partially funded by the National Institutes of Health (HL68878, HL89544, and HL92421). K.J.Y. and J.Z. are supported by the American Heart Association National Scientist Development Grant 0630209N and 0835237N, respectively. M.H. is supported by a postdoctoral fellowship from the National Institutes of Health (T32 HL007853). Y.E.C. is an established investigator of the American Heart Association (0840025N).

REFERENCES

Bartel DP. MicroRNAs: genomics, biogenesis, mechanism, and function. Cell 2004;116:281–97. [PubMed: 14744438]

Bartel DP. MicroRNAs: target recognition and regulatory functions. Cell 2009;136:215–33. [PubMed: 19167326]

Bartel DP, Chen CZ. Micromanagers of gene expression: the potentially widespread influence of metazoan microRNAs. Nat Rev Genet 2004;5:396–400. [PubMed: 15143321]

Care A, et al. MicroRNA-133 controls cardiac hypertrophy. Nat Med 2007;13:613–8. [PubMed: 17468766]

Chen J, et al. Suppression of endogenous bcl-2 expression by antisense treatment exacerbates ischemic neuronal death. J Cereb Blood Flow Metab 2000;20:1033–9. [PubMed: 10908036]

Cimmino A, et al. miR-15 and miR-16 induce apoptosis by targeting BCL2. Proc Natl Acad Sci U S A 2005;102:13944–9. [PubMed: 16166262]

Dharap A, et al. Transient focal ischemia induces extensive temporal changes in rat cerebral microRNAome. J Cereb Blood Flow Metab 2009;29:675–87. [PubMed: 19142192]

Frankel LB, et al. Programmed cell death 4 (PDCD4) is an important functional target of the microRNA miR-21 in breast cancer cells. J Biol Chem 2008;283:1026–33. [PubMed: 17991735]

Goldstein LB, et al. Primary prevention of ischemic stroke: A statement for healthcare professionals from the Stroke Council of the American Heart Association. Stroke 2001;32:280–99. [PubMed: 11136952]

Hata R, et al. Targeted disruption of the bcl-2 gene in mice exacerbates focal ischemic brain injury. Metab Brain Dis 1999;14:117–24. [PubMed: 10488913]

Hayashita Y, et al. A polycistronic microRNA cluster, miR-17–92, is overexpressed in human lung cancers and enhances cell proliferation. Cancer Res 2005;65:9628–32. [PubMed: 16266980]

Hebert SS, et al. Loss of microRNA cluster miR-29a/b-1 in sporadic Alzheimer's disease correlates with increased BACE1/beta-secretase expression. Proc Natl Acad Sci U S A 2008;105:6415–20. [PubMed: 18434550]

Jeyaseelan K, et al. MicroRNAs as therapeutic targets in human diseases. Expert Opin Ther Targets 2007;11:1119–29. [PubMed: 17665982]

Jovanovic M, Hengartner MO. miRNAs and apoptosis: RNAs to die for. Oncogene 2006;25:6176–87. [PubMed: 17028597]

Kalache A, Aboderin I. Stroke: the global burden. Health Policy Plan 1995;10:1–21. [PubMed: 10141620]

Ketting RF, et al. Dicer functions in RNA interference and in synthesis of small RNA involved in developmental timing in C. elegans. Genes Dev 2001;15:2654–9. [PubMed: 11641272]

Kim J, et al. A MicroRNA feedback circuit in midbrain dopamine neurons. Science 2007;317:1220–4. [PubMed: 17761882]

Kim VN. MicroRNA biogenesis: coordinated cropping and dicing. Nat Rev Mol Cell Biol 2005;6:376–85. [PubMed: 15852042]

Kosik KS. The neuronal microRNA system. Nat Rev Neurosci 2006;7:911–20. [PubMed: 17115073]

Krutzfeldt J, Stoffel M. MicroRNAs: a new class of regulatory genes affecting metabolism. Cell Metab 2006;4:9–12. [PubMed: 16814728]

Kuhn DE, et al. Experimental validation of miRNA targets. Methods 2008;44:47–54. [PubMed: 18158132]

Lee Y, et al. MicroRNA genes are transcribed by RNA polymerase II. EMBO J 2004;23:4051–60. [PubMed: 15372072]

Linnik MD, et al. Expression of bcl-2 from a defective herpes simplex virus-1 vector limits neuronal death in focal cerebral ischemia. Stroke 1995;26:1670–4. discussion 1675. [PubMed: 7544927]

Love S. Apoptosis and brain ischaemia. Prog Neuropsychopharmacol Biol Psychiatry 2003;27:267–82. [PubMed: 12657366]

Martinou JC, et al. Overexpression of BCL-2 in transgenic mice protects neurons from naturally occurring cell death and experimental ischemia. Neuron 1994;13:1017–30. [PubMed: 7946326]

Meng F, et al. MicroRNA-21 regulates expression of the PTEN tumor suppressor gene in human hepatocellular cancer. Gastroenterology 2007;133:647–58. [PubMed: 17681183]

Mott JL, et al. mir-29 regulates Mcl-1 protein expression and apoptosis. Oncogene 2007;26:6133–40. [PubMed: 17404574]

Paxinos G, et al. Bregma, lambda and the interaural midpoint in stereotaxic surgery with rats of different sex, strain and weight. J Neurosci Methods 1985;13:139–43. [PubMed: 3889509]

Schellinger PD, et al. An update on thrombolytic therapy for acute stroke. Curr Opin Neurol 2004;17:69–77. [PubMed: 15090880]

Schickel R, et al. MicroRNAs: key players in the immune system, differentiation, tumorigenesis and cell death. Oncogene 2008;27:5959–74. [PubMed: 18836476]

Stapf C, Mohr JP. Ischemic stroke therapy. Annu Rev Med 2002;53:453–75. [PubMed: 11818485]

Sullivan CS, Ganem D. MicroRNAs and viral infection. Mol Cell 2005;20:3–7. [PubMed: 16209940]

Sun Y, et al. Adeno-associated virus-mediated delivery of BCL-w gene improves outcome after transient focal cerebral ischemia. Gene Ther 2003;10:115–22. [PubMed: 12571640]

Swanson RA, et al. A semiautomated method for measuring brain infarct volume. J Cereb Blood Flow Metab 1990;10:290–3. [PubMed: 1689322]

Vemuganti R, et al. Inhibition of intercellular adhesion molecule-1 protein expression by antisense oligonucleotides is neuroprotective after transient middle cerebral artery occlusion in rat. Stroke 2004;35:179–84. [PubMed: 14657453]

Webster KA, et al. Redox stress and the contributions of BH3-only proteins to infarction. Antioxid Redox Signal 2006;8:1667–76. [PubMed: 16987020]

Wiemer EA. The role of microRNAs in cancer: no small matter. Eur J Cancer 2007;43:1529–44. [PubMed: 17531469]

Wienholds E, Plasterk RH. MicroRNA function in animal development. FEBS Lett 2005;579:5911–22. [PubMed: 16111679]

Yang GY, et al. Overexpression of interleukin-1 receptor antagonist in the mouse brain reduces ischemic brain injury. Brain Res 1997;751:181–8. [PubMed: 9099804]

Yin KJ, et al. ATM gene regulates oxygen-glucose deprivation-induced nuclear factor-kappaB DNA-binding activity and downstream apoptotic cascade in mouse cerebrovascular endothelial cells. Stroke 2002a;33:2471–7. [PubMed: 12364740]

Yin KJ, et al. Matrix metalloproteinases expressed by astrocytes mediate extracellular amyloid-beta peptide catabolism. J Neurosci 2006a;26:10939–48. [PubMed: 17065436]

Yin KJ, et al. Protein phosphatase 2A regulates bim expression via the Akt/FKHRL1 signaling pathway in amyloid-beta peptide-induced cerebrovascular endothelial cell death. J Neurosci 2006b;26:2290–9. [PubMed: 16495456]

Yin KJ, et al. Amyloid-beta induces Smac release via AP-1/Bim activation in cerebral endothelial cells. J Neurosci 2002b;22:9764–70. [PubMed: 12427831]

Youle RJ, Strasser A. The BCL-2 protein family: opposing activities that mediate cell death. Nat Rev Mol Cell Biol 2008;9:47–59. [PubMed: 18097445]

Yuan J. Neuroprotective strategies targeting apoptotic and necrotic cell death for stroke. Apoptosis 2009;14:469–77. [PubMed: 19137430]

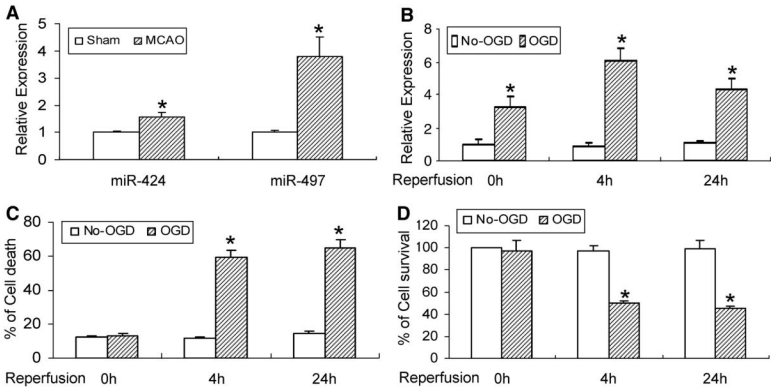

Figure 1.

Altered expression of miR-497 in mouse brain after focal cerebral ischemia and in OGD-induced neuronal death. (A) The expression of cerebral miR-497 and miR-424 is increased in mice subjected to transient MCAO and 24h of reperfusion. (B) OGD causes a time-dependent elevation in miR-497 levels, increasing at the starting point of recovery following 3h of OGD exposure and persisting at least to the 24h recovery time point after OGD. (C, D) Exposure to OGD also results in obvious mouse N2A cell death detected by LDH (C) and MTT (D) assays. OGD-induced neuronal loss is present at the 4h recovery time point, and persisted to at least the 24h recovery time point after 3h OGD. *P<0.05 vs non-OGD controls. Representative data from 3 separate experiments with similar results are shown.

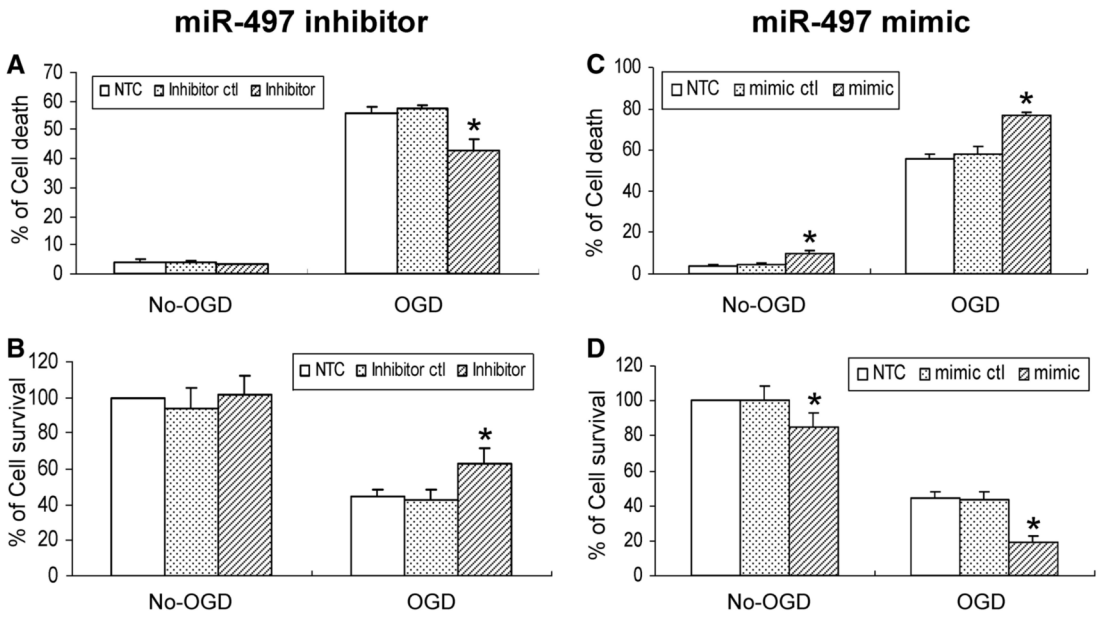

Figure 2.

miR-497 regulation of mouse N2A cell death after OGD. A miR-497 inhibitor, but not miR-497 inhibitor control attenuates OGD-induced neuronal death detected by LDH (A) and MTT (B) assays. In contrast, a miR-497 mimic, but not mimic control aggravates neuronal loss in both non-OGD and OGD conditions (C, D). * $P<0.05$ vs mimic or inhibitor control. Results shown are representative of 3 separate experiments with similar results.

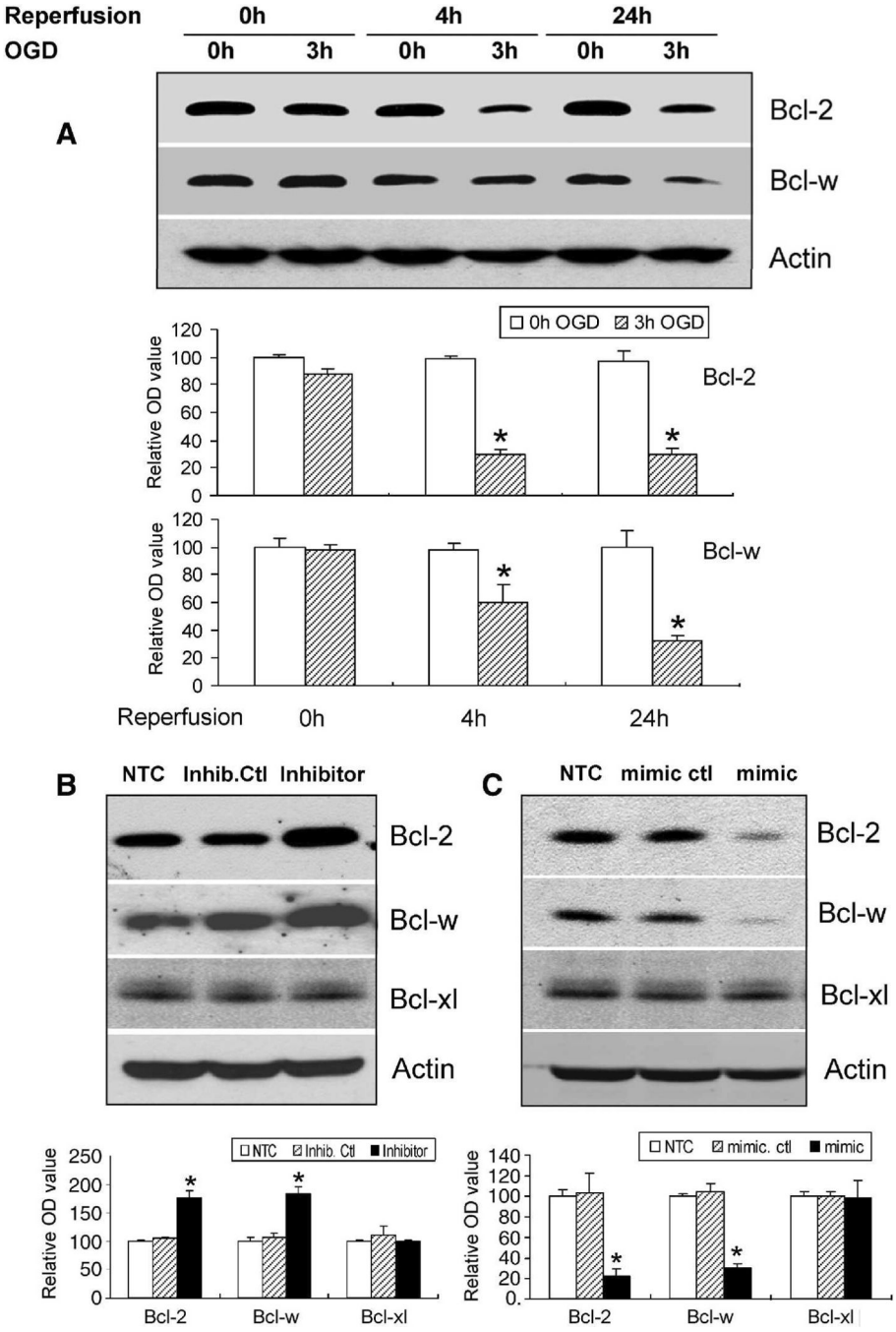

Figure 3.

Bcl-2 and bcl-w are target genes of miR-497 in mouse N2A cells. The protein levels of bcl-2 and bcl-w are significantly decreased after OGD. This decrease in expression is evident at the 4h recovery time point after 3h of OGD and persisted up to the 24h recovery time point after OGD (A). Treatment of mouse N2A cells with a miR-497 inhibitor effectively increases both bcl-2 and bcl-w levels after OGD (B). In contrast, a miR-497 mimic reduces the protein expression of bcl-2 and bcl-w after OGD (C). The expression of bcl-xl, one bcl-2 family protein, is not affected in mouse N2A cells after treatment with either a miR-497 mimic or inhibitor. The miR-497 mimic and inhibitor controls have no effect on the expression of bcl-2 and bcl-w. Data shown in top panels of figure 3A, B, C are representative of 3 separate experiments

with similar results. Quantitative analysis of data in bottom panels of Fig 3A, B, C is expressed as mean ± SD. *$p < 0.05$ versus non-OGD controls or mimic and inhibitor controls.

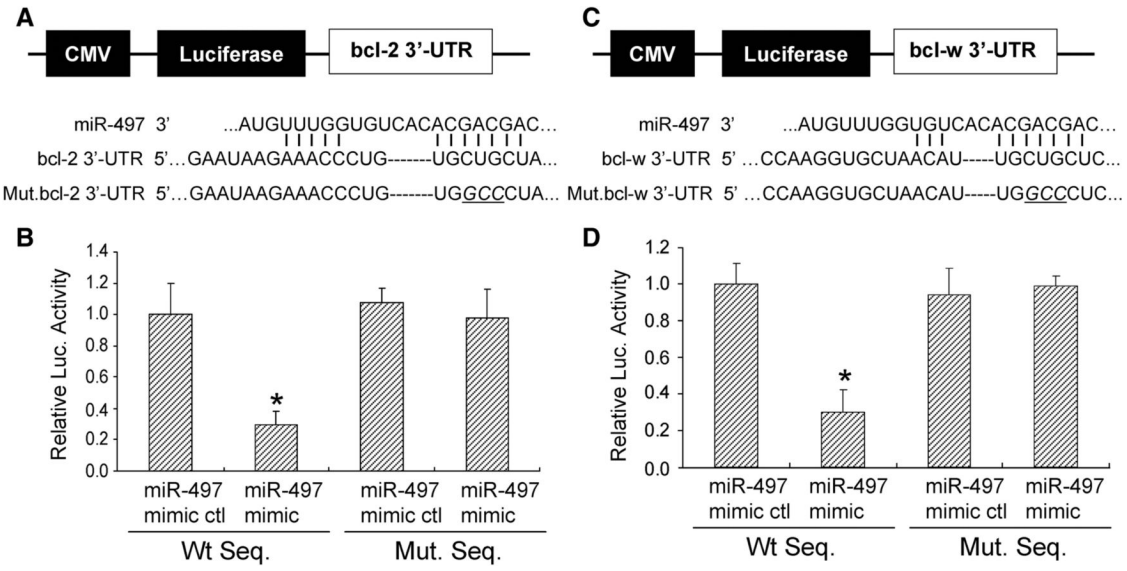

Figure 4.

A miR-497 binding site within the 3'-UTRs of bcl-2 and bcl-w mediates miR-497 translational repression. (A, C Top) Design of a miR-497 reporter vector containing a CMV-driven expression of a luciferase cDNA fused to a bcl-2 3'-UTR (pMIR-bcl2-3'-UTR), bcl-w 3'-UTR (pMIR-bclw-3'-UTR), mutated bcl-2 3'-UTR (pMIR-bcl2-m3'-UTR) or mutated bcl-w 3'-UTR (pMIR-bclw-m3'-UTR). MiR-497 and the miR-497-binding site in the 3'UTRs of bcl-2 (A bottom) and bcl-w (C bottom) are shown. (B, D) The 3'-UTR of bcl-2 and bclw mediate miR-497 control of bcl-2 and bcl-w expression. Mouse N2A cells were transfected with a pMIR-bcl-2-3'-UTR, pMIR-bcl-w-3'-UTR, pMIR-bcl-2-m3'-UTR, or pMIR-bcl-w-m3'-UTR respectively. The cells were also cotransfected with a miR-497 mimic or mimic control. Compared to the mimic control, the miR-497 mimic decreases expression of luciferase containing a wild type miR-497 binding site (*Left 2 columns*) but not a mutant binding site (*Right 2 columns*). Data are expressed as mean ± SEM. * $P<0.05$ vs mimic control. Results shown are representative of 3 separate experiments with similar results.

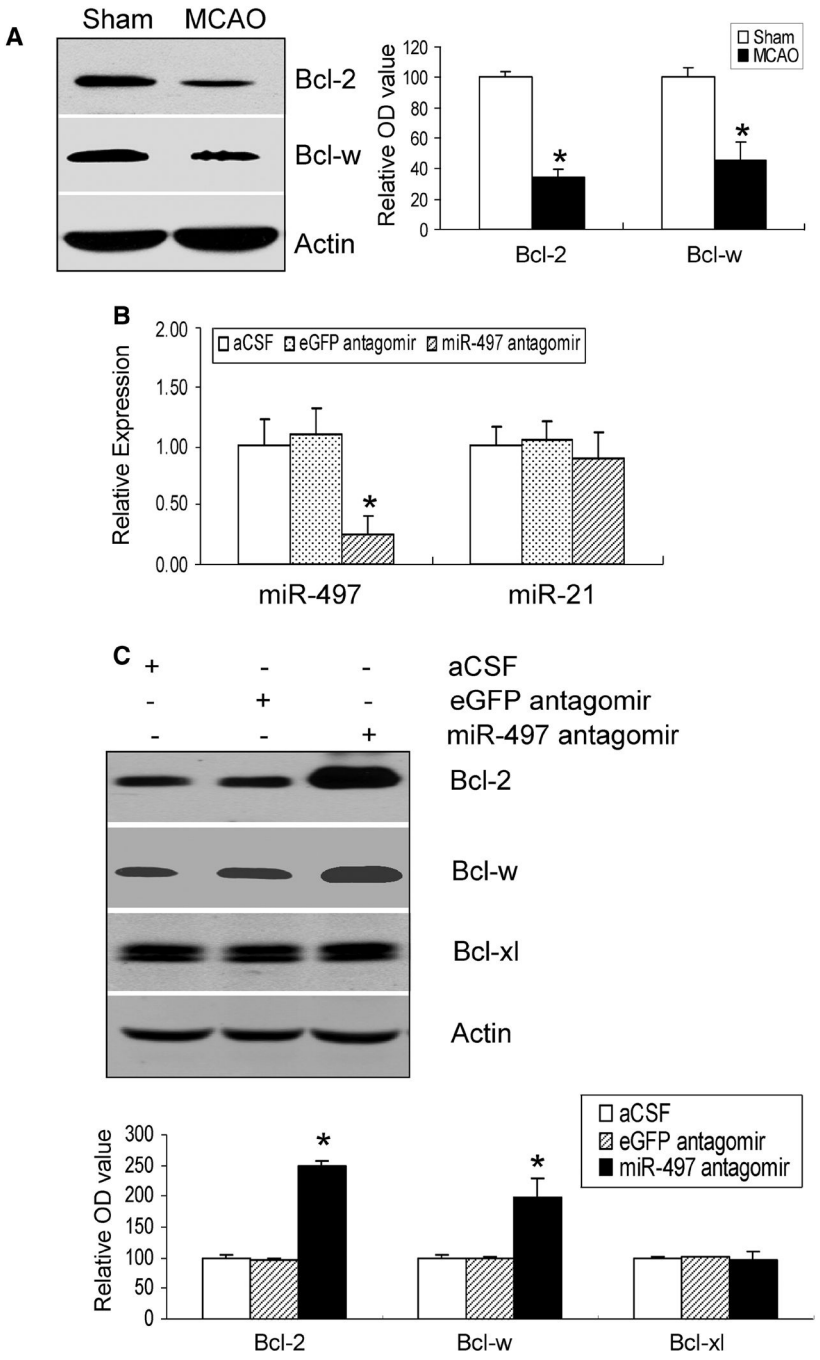

Figure 5.

Bcl-2 and bcl-w are miR-497 target genes in mouse cerebral cortex after transient focal cerebral ischemia. Bcl-2 and bcl-w are downregulated following 24 h-reperfusion after 1h MCAo (A). Mini-pump assisted-cerebroventricular infusion of a miR-497 antagomir effectively inhibits cerebral miR-497 expression (B) and significantly enhances bcl-2 and bcl-w protein levels (C) in mouse cerebral cortex at the 24 h reperfusion time point after 1h MCA occlusion. In contrast, administration of an eGFP mRNA antagomir or artificial CSF (aCSF) has no effect on the expression of miR-497 and its two target proteins. Of note, the expression levels of bcl-xl, another member of the bcl-2 family is not affected in the ischemic cerebral cortex after treatment with the miR-497 antagomir. Quantitative analysis of data with representative blots

shown in Fig 5A, C are in the respective bottom panels. Data are expressed as mean ± SD from 3 separate experiments. * denotes $p < 0.05$ versus sham or eGFP antagomir group.

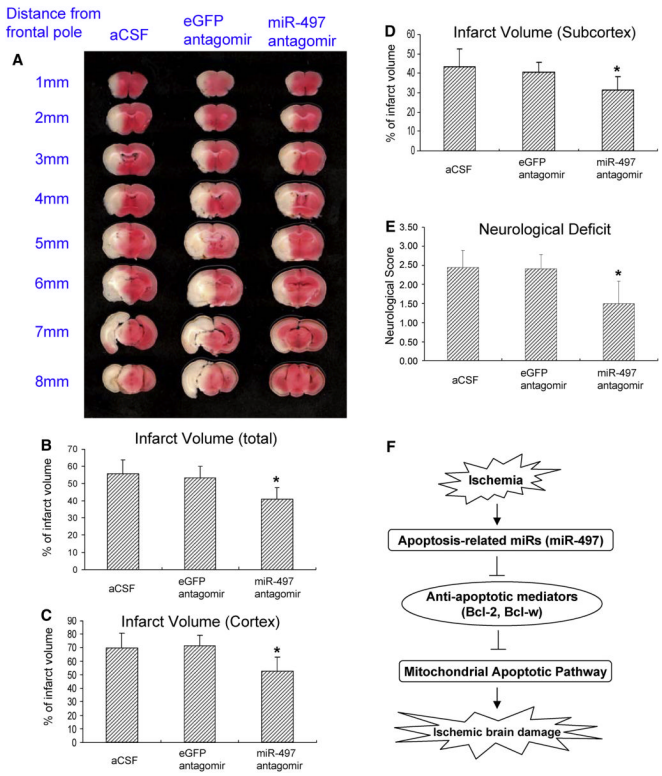

Figure 6.

The effect of miR-497 inhibition on ischemic infarction and neurological outcome. Mice were pretreated with a miR-497 antagomir, eGFP mRNA antagomir or artificial CSF (aCSF) for 48h via mini-pump assisted-cerebroventricular infusion, and then subjected to 1h MCA occlusion and 24h-reperfusion. 2% TTC-stained coronal sections were shown at different brain levels posterior to the frontal pole (A). Quantitative analysis was made on brain infarct volume in total (B), cortex (C), subcortex (D) areas (n=8) and neurological deficits (E) (n=11) in mice after stroke. In comparison to the controls, inhibition of the miR-497antagomir significantly attenuates ischemic infarct volume and improves behavioral outcome. Data are expressed as mean ± SD. * $p < 0.05$ vs the eGFP mRNA antagomir or artificial CSF group. (F) Schematic representation of miR-497 regulation of anti-apoptotic bcl-2 and bcl-w during ischemia-induced cell death signaling. In mouse brain, ischemic stimuli induce microRNA dysfunction, featuring activated miR-497 expression. miR-497 binds to the 3'-UTR region of bcl-2 and bcl-w, and further inhibits their activities by post-transcriptional gene silencing, thereby resulting in ischemic neuronal loss via mitochondrial apoptotic signaling.